R. Shafer/January 2, 1979

Study of Eddy Current Effects in Energy Doubler Dipole Magnets

Introduction

Eddy currents are generated in metallic components of the energy doubler dipole magnets whenever the excitation current is time dependent. The effects of the eddy currents are several: They can dissipate power in cryogenic components and add heat load to the cryogenic system; they can distort magnetic fields, both by retardation and by attenuation; and they can damp transmission-line type resonances in large strings of magnets.

The purpose of this note is to derive a simple electrical circuit model for the eddy current losses, to compare the model with measurements on many magnets, both warm and superconducting, and in various stages of assembly, to establish component values in the model and to pinpoint the parts which are the major contributors to the eddy current losses. The results are compared to AC power loss measurements made on ramped superconducting magnets, and some comments and suggestions are made in relation to what effects to look for in AC magnetic field measurements, and possible limitations of the present magnetic field measuring equipment for AC magnetic measurements. The study of the transmission line characteristics of large strings of magnets will be described in another note.

Electrical Model

The electrical equivalent circuit for eddy current losses (core losses) in electrical equipment (e.g. transformers) is

essentially a mutual inductance coupled secondary with a dissipative load:

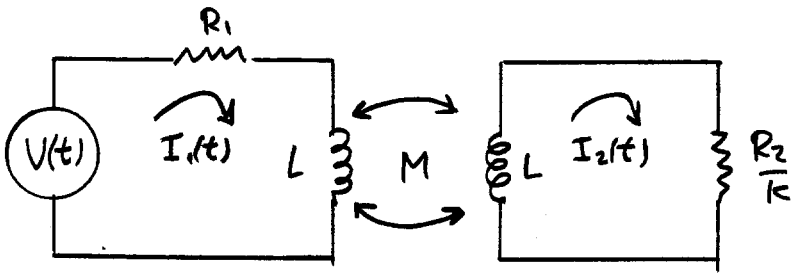

$M^2 = KL^2$

The inductance of the primary and secondary circuits are chosen to be equal, and the eddy current load is chosen to be R_2/K, without loss of generality, and for reasons which will shortly be apparent.

The equations governing this circuit are:

$$V(t) = (R_1 + j\omega L) I_1(t) + j\omega M I_2(t)$$

$$0 = \left(\frac{R_2}{K} + j\omega L\right) I_2(t) + j\omega M I_1(t) \qquad [1]$$

Eliminating $I_2(t)$ and substituting $KL^2 = M^2$ leads to the following form for the impedance at the circuit as seen from the primary:

$$Z = \frac{V(t)}{I_1(t)} = R(\omega) + j\omega L(\omega) \qquad [2]$$

$$R(\omega) = R_1 + \frac{KL\tau\omega^2}{1+\omega^2\tau^2} \; ; \; L(\omega) = (1-K)L + \frac{KL}{1+\omega^2\tau^2} \qquad \tau = \frac{KL}{R_2}$$

this equation is precisely the equation for the impedance of the following equivalent circuit:

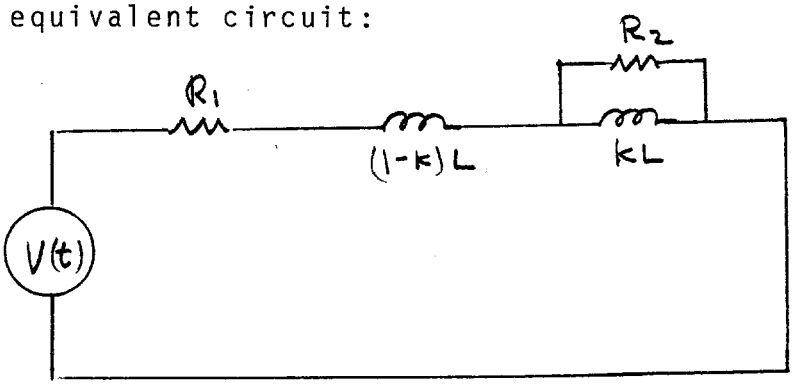

The purpose of using this equivalent circuit is to provide some additional insight into physicially what happens when eddy currents are present in a magnet.

The DC inductance is L. However, if an AC signal is applied, and the frequencies approach $\omega \sim \frac{1}{\tau}$ the inductance of the magnet is reduced. For frequencies where $\omega >> 1/\tau$, the inductance again becomes independent of frequency, but is reduced by that portion which is coupled to the eddy currents. The DC resistance, R_1, is increased by a resistance proportional to ω^2 for $\omega << 1/\tau$. As will be seen in the actual measurements, $w_{\tau} << 1$ for ramping the magnets, so the eddy current losses are proportional to $kL\tau w^2$. In actuality, there are many eddy current losses, and hence

$$kL\tau\omega^2 \longrightarrow \sum_i k_i L\tau_i \omega^2$$

Nevertheless, specific structures in the magnet can be approximately represented by specific values of $kL\tau$.

As the resistance $R(\omega)$ is intimately related to the change in inductance with frequency, the eddy current losses at some frequency $w << 1/\tau_{max}$ can be calculated from actual inductance measurements:

$$R(\omega) = R_1 - \frac{2\omega^2}{\pi}\int_{1/\tau_{max}}^{\infty} \frac{1}{\omega'} \frac{2L(\omega')}{2\omega'} d\omega' \qquad [3]$$

where the integral is model independent and carried out by numerically integrating experimental measurements.

This integral relation is a direct result of dispersion relations and derived in the Appendix. Hence large inductance changes at low frequencies represent the dominant eddy current losses. A loss at 10% of the total inductance at 10 Hz is worse than a loss of 50% at 300 Hz for example.

Observable Effects of Eddy Currents

Consider the equivalent circuit model (without coil resistance):

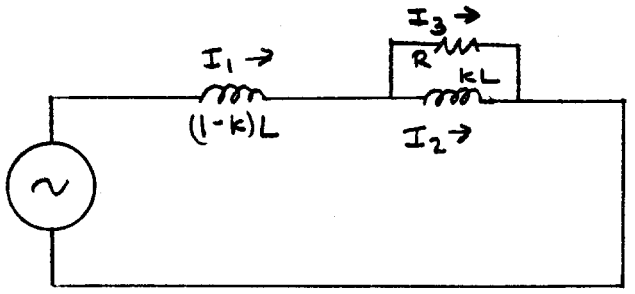

Consider sinewave exitation $I_1 = I_0 e^{i\omega t}$

$$I_1 = I_2 + I_3$$

$$I_3 R = j\omega kL I_2$$

$$\therefore I_2 = \frac{R I_1}{R + j\omega kL} = \frac{I_1}{1 + j\omega\tau} = \frac{(1 - j\omega\tau) I_1}{1 + \omega^2\tau^2}$$

$$= \frac{e^{-j\omega\tau} I_1}{[1 + \omega^2\tau^2]^{1/2}} = \frac{I_0 e^{+j\omega(t-\tau)}}{[1 + \omega^2\tau^2]^{1/2}} \qquad [4]$$

Hence for sinewave exitation there is both an attenuation as well as a retardation of the current (and the corresponding magnetic field) coupled to the eddy current losses. The retardation is independent of frequency and is easily observed (this was measured with a magnetic pickup loop in the bore of a typical ED magnet for example).

A more realistic example is the case of an applied voltage step resulting in a constant dI/dt.

Using the Laplace variable $s = \alpha + iw$ we can write down the following equations for the above circuit:

$$V(s) = \left[(1-k)Ls + \frac{kRLs}{R+kLs}\right] I_1(s)$$

$$I_1(s) = I_2(s) + I_3(s)$$

$$R\, I_3(s) = Ls\, I_2(s) \qquad [5]$$

Hence

$$I_1(s) = \frac{R + kLs}{RLs + (1-k)kL^2s^2}\, V(s) \qquad [6]$$

$$I_2(s) = \frac{R}{RLs + (1-k)kL^2s^2}\, V(s)$$

We now consider $V(t) = 0 \quad t<0$

$$V(t) = V_0 \quad t\geq 0$$

the Laplace transform of this is $V(s) = \frac{V_0}{S}$

using $\tau' = \frac{(1-k)kL}{R} = (1-k)\tau$ and $\tau = \frac{kL}{R}$:

$$I_1(s) = \frac{V_0}{L\tau'}\left[\frac{1}{s^2\left(\frac{1}{\tau'}+s\right)}\right] + \frac{kV_0}{R\tau'}\left[\frac{1}{s\left(\frac{1}{\tau'}+s\right)}\right]$$

$$I_2(s) = \frac{V_0}{L\tau'}\left[\frac{1}{s^2\left(\frac{1}{\tau'}+s\right)}\right] \qquad [7]$$

Carrying out the transformation:

$$I_1(t) = I_o + \frac{V_o}{L}\left[t - \tau'(1-e^{-t/\tau'})\right] + \frac{kV_o}{R}\left[1-e^{-t/\tau'}\right] \qquad [8]$$

$$I_2(t) = I_o + \frac{V_o}{L}\left[t - \tau'(1-e^{t/\tau'})\right]$$

where I_o = the DC current flowing at t=o

For times large compared to τ':

$$I_1(t) = I_o + \frac{V_o}{L}\left[(t - \tau')\right] + \frac{KV_o}{R}$$

$$= I_o + \frac{V_o}{L}(t - \tau' + \tau) \qquad \text{since } \frac{V_o}{L} = \frac{dI_1}{dt};$$

$$I_2(t) = I_1(t) - \tau\frac{dI_1}{dt}$$

$$I_2(t) = I_o + \frac{V_o}{L}(t - \tau') \qquad [9]$$

We notice again that I_2 is retarded from the external current I_1 by an amount τ, but not associated with any attenuation as there was in the sinewave exitation. In the actual case τ is space dependent; i.e. τ can vary from point to point in the magnetic aperture and cause distortions of the magnetic field. These distortions are of the order of equivalent superimposed currents $\delta\tau \frac{dI}{dt}$ exciting various multipoles, where $\delta\tau$ is the variation of τ within the aperture. It is important to note that $\frac{dI_2(t)}{dt} = \frac{dI_1(t)}{dt}$ under steady state ramping conditions, leading to the observation that "flip coil" type magnetic field measuring equipment should not be used to measure AC magnetic fields except under very special conditions. This measuring technique is insensitive to distortions caused by retardation.

A computer simulation of the retardation effect for a typical case is shown in figure 1. It is interesting to note that the steady-state slope of the externally applied current leads the ideal current (i.e. for the same circuit without eddy currents) by an amount $\tau - \tau'$. Another way of saying this is that the inductance changes during ramping.

The difference between $I_1(t)$ and $I_2(t)$ represents the current flowing into R, the eddy current losses. If we consider a ramping cycle to some current I_{max} from 0 current and back with a constant dI/dt we can calculate the energy loss per cycle:

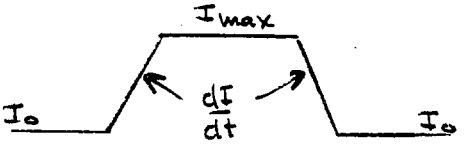

$$W = \oint \left(\frac{V_o}{L}\tau\right)^2 R\, dt = 2\left(\frac{dI}{dt}\tau\right)^2 \frac{kL}{\tau} \quad \frac{I_{max}}{dI/dt}$$

$$= 2\, kL\tau\, I_{max} \frac{dI}{dt} \quad \text{Joules/cycle} \qquad [10]$$

As shown above, the value of $kL\tau$ for an actual magnet can be obtained by measuring the frequency dependence of the inductance and integrating:

$$W = -\frac{4}{\pi} I_{max} \frac{dI}{dt} \int_{1/\tau_{max}}^{\infty} \frac{1}{\omega'} \frac{2L(\omega')}{2\omega'} d\omega' \quad \frac{\text{Joules}}{\text{cycle}} \qquad [11]$$

as well as by directly measuring the real component of $Z(\omega)$.

Measurement Technique

Measurements have been made in two ways. The first method employed was to use the Hewlett Packard Model 4800 Vector Impedance meter, which yields the magnitude and angle of the impedance directly. This method was satisfactory for use with dipole magnets with iron yokes, but was subject to considerable stray electrical interference when the yoke was not present. Unshielded dipole coils seem to be excellent antennas,

and as the signal level employed by the vector impedance meter is about 2 millivolts, its sensitivity to stray electrical interference is high.

The second method used was to connect a precision resistor decade box in series with the dipole, and excite the circuit with a sinewave signal generator for frequencies 10 Hz < f < 5 kHz. Voltages across the resistor, the dipole, and the combination were read using a digital voltmeter, and the real and imaginary components of the dipole impedance were calculated using the trig relations of the complex impedance. As this method employed much higher signal levels (about 40 milliamps) it was much less sensitive to electrical interference. In addition, the precision of the measurements obtained by this method seems to be consistently better than ±1% or ±.05 ohms for both the real and imaginary components for frequencies above 30 Hz, with some degradation in the 10 Hz - 30 Hz range. The particular digital voltmeter used precluded making measurements below 10 Hz.

In all, about 20 dipoles have been measured, in many stages of assembly, and at both room temperature and superconducting when possible. Reproducability of different coils yielding similar results under similar conditions was quite good, and for this reason only some of the results will be presented. This also allows comparing the results of measuring different coils under different conditions, and interpreting the differences as being a result of the different conditions rather than different coils. In those cases where similar measurements were made using the two measuring techniques, the results were in agreement.

Eddy Current Losses in Stainless Steel Collars, Cyrostat, and Bore Tube

Figures 2A and 2B show the measured real and imaginary components of the dipole impedance for the three following assemblies:

Coil No	Temperature	ss cryostat	Bore Tube	Location
140	room temp	none	none	Lab 5
144	room temp	yes	none	Indust. Bldg 3
154	room temp	yes	yes	Indust. Bldg 1

In Figure 2B, the inductance of coil No. 140 is shown as being roughly constant up to about 1 kHz, at which point it begins to rise. This rise is thought to be due to turn-to-turn capacitance in the coil, which gives rise to a pole in the reactance of the form $1-\omega^2 LC$. As this can very from coil to coil, the ability to distinguish other characteristics between coils is diminished somewhat above 1 or 2 kHz. The inductance of coil No. 144 and 154 both begin to drop noticeably above 100 Hz, and are in rough agreement up to about 1 kHz, where coil No. 154 (with the bore tube) starts decreasing rapidly relative to coil No. 144. The resistive component of the impedance in Figure 2A (with the DC. resistance subtracted) shows a ω^2 dependence for all 3 coils up to about 200 Hz, at which point both coils with the ss cryostat start to "saturate", while the bare coil (140) continues upward with the ω^2 dependence.

These results may be interpreted in the light of equation (2) as follows. Coil No. 140 (bare) represents the losses in the ss collar (and perhaps the coil itself) with a value of $\omega\tau \ll 1$ for all frequencies measured. Correspondingly, we would not expect to see any change in the inductance.

Coils 144 and 154 both show a decrease in inductance and a saturation in the resistance, which can be interpreted as $\omega\tau \geq 1$. At high frequencies we therefore expect the resistance $R(\omega)$ of coils 144 and 154 to approach the resistance of coil 140 plus a constant, the constant being due to the ss cryostat and bore tube. At frequencies $\leq$100 Hz it is possible to estimate the relative contributions of the ss collars, cryostat, and bore tube, assuming all coils are equivalent and that none of the losses are from the coil itself:

% loss in ss cryostat*	80%
ss bore tube	12%
ss collars	8%

* the nitrogen shield probably contributes about 40% of this

the addition of the iron yoke will certainly affect these relative contributions, but qualitatively it can be stated that the most significant eddy current loss is in the cryostat*, and not in the collars or bore tube.

When the yoke is installed, the inductance increases by about 30% and when the stainless is cooled to 4°K the resistivity decreases somewhat (about 20%) so we can expect the coefficient of ω^2 for these eddy current losses to increase by roughly a factor $1.2 \times (1.3)^2 \approx 2.0$.

Warm Vs Superconducting Measurements in Lab 5

Figure 3A and B show the resistance and inductance respectively of coil 159 (a bare coil without either ss cryostat or bore tube) installed in the aluminum dewar in Lab 5, both warm and superconducting. Similar results were obtained for coil 158 (not shown). In figure 3B (note expanded scale) the inductance of the warm coil is reduced about 3 mHy from the bare coil (see Fig. 2B) due to the presence of the 12" diameter 1/4" wall aluminum dewar which "traps" the flux lines inside . This apparently occurs at very low frequencies, as the resistive component for the warm coil deviates from the expected ω^2 behavior at low frequencies, and approaches the "bare" coil (140 in figure 2B) at large ω. (It should be noted that the aluminum dewar does include a stainless sleeve about 9" diameter, the effect at which should be qualitatively similar to the ss cryostat in Figs 2A and B but of much smaller magnitude as it is 1/4th as thick, and is a larger diameter. In any case, it should only contribute a ω^2 term at low frequencies.

It is apparent for the superconducting coil that there is a somewhat higher resistive loss at low frequencies, coupled with some missing inductance (about 2 mHy at 10 Hz, increasing to about 4 mHy at 1kHz). Interpretation of this as to skin effect etc., is open to conjecture and will be discussed after the results of fully assembled magnets are presented.

Measurements of Warm Vs Superconducting ED Dipoles

Figure 4A and B present resistance and inductance measurements on dipole PCA-148, a fully assembled magnet on a test stand in Industrial Bldg. 1. In addition to being fully assembled (i.e. with cryostat, bore tube, and yoke), there was in

addition a "warm bore" assembly installed to be used in conjunction with magnetic measurements. Based on the contribution of the normal bore tube, this probably would increase the total eddy current losses another 25% or so.

In Figure 4A, the straight line is the low frequency limit predicted by the dispersion relation (equation 3) using the inductance measurements for PCA-148 (superconducting) in Figure 4B, and assuming that $\frac{\partial L(\omega)}{\partial \omega} = 0$ for $\omega < (2\pi \times 10$ Hz). At high frequencies R(w) shows some signs of saturation, as it approaches a constant plus the contribution from the stainless steel collars. The line shown is a factor of two above that measured in coil 140 at room temperature, to allow for the increased inductance as well as the decreased resistivity of the stainless. The slight increase in R(w) below 100 Hz, and decrease at 1000 Hz in the superconducting value as compared to the room temperature value may be related to the change in resistivity of stainless, as the net effect is to increase the time constant τ, which increases the coefficient of ω^2 which is proportional to $1/\tau$.

In Figure 4B, the inductance measurements are shown. The very large drop in inductance between 100 and 1000 Hz is probably due mainly to the stainless steel cryostat, as discussed earlier. The similarity of shape of the warm and superconducting curves imply that the change in resistivity is not large. The room temperature value of inductance is about 48.2 mHy in the 10-30 Hz region, and is possibly the dc value. Theoretical calculations yield a somewhat higher value, about 49.6 mHy. The inductance loss when the dipole becomes superconducting is roughly 3 mHy for f = 30 Hz, increasing to about 5 mHy in the 100-300 Hz region. This rise in lost inductance with frequency could be partially explained by a change in resistivity in the stainless cryostat, causing the curve to be shifted to lower frequencies, but also could be the same effect seen in figure 3B.

DC Inductance Loss at Superconducting Temperatures

A possible explanation at the loss of inductance at superconducting temperatures is the following: the superconducting ribbon occupies a certain fraction of the volume of the dipole in which the magnetic energy is stored. Exclusion of magnetic energy from any part of this volume for any reason will be reflected in a corresponding loss of inductance. If this loss of inductance is frequency dependent, there will be a corresponding increase in the AC losses, based on the prediction of the dispersion relations. If, however, the DC inductance is also reduced correspondingly, then there will be no increase in the AC losses.

By volume, the superconducting ribbon is composed of copper (61%), superconducting filaments (34%), and voids between the strands (5%). Due to the superconducting nature of the Nb-Ti filaments, this volume is excluded from storing any magnetic energy (below critical field values) even at DC*, hence leading to a DC loss of inductance. At higher frequencies, as the skin effect in the .025" strands becomes important, the volume occupied by the copper will also become important, leading to an additional frequency dependence of inductance loss (slightly over a factor of 2). We may see these effects in both figure 3B and 4B.

As only a small fraction of volume is occupied by voids, low resistivity contacts between strands in the ribbon (eg STABRITE) probably would not change the total lost inductance much, but would shift the inductance loss to lower frequencies due to the

*Assuming type II superconductors approach type I characteristics (perfect diamagnetism) at low exitation levels.

relatively larger dimensions of the ribbon vs the individual strands, as the inductance change due to skin depth depends both on frequency and cross-sectional dimensions. This shift toward lower frequencies would increase the AC losses in the dipoles as they are proportional to $\frac{1}{\omega}\frac{2L(\omega)}{2\omega}$ (see equation 3). It is quite possible that careful inductance measurements could shed some light on the stabrite vs ebanol insulation problem in the magnets. A very useful number which would help in this matter is knowledge of what the DC inductance loss of a superconducting dipole is, as it would tell us whether we have reached it at 10 Hz in PCA 148.

Predictions of AC Losses

The predicted asymptotic value of R(w) in PCA-148 from figure 4A is $R(w) = 2.1 \times 10^{-5}\ \omega^2$. If we reduce this by 25% to correct for the "warm bore" assembly, we get $R(w) = 1.6 \times 10^{-5}\ \omega^2$. Using equation 10 and 11 to predict the eddy current portion of losses in the 2000 A ramp studies we get

$$W = 2 \times 1.6 \times 10^{-5} \times 2000\ A \times 400\ A/sec$$

$$= 26\ Joules/cycle\ at\ 400\ A/sec.$$

This is in resonable agreement with the non-hysteresis portion of AC losses measured. Part of this is in the nitrogen shield.

Phase Shift and Retardation

Using a value of $R(\omega) = 1.6 \times 10^{-5} \omega^2$ and an estimated kL of .6 x 45 mH leads to a τ in the vicinity of the cryostat of about 0.6 milliseconds. As a large fraction of the field lines in the bore tube must also penetrate the cyrostat, we would expect a similar phase shift there as well. A simple test on a warm magnet in Industrial Bldg 1 yielded a τ of 300 ±20 μsec inside the bore tube. No substantial positional dependence exceeding ±20 μsec was seen. At a ramp rate of 400 amps/sec, this corresponds to

$\tau \frac{dI}{dt}$ = 0.12 amps, and $\Delta\tau \frac{dI}{dt}$ = 0.008 amps. The latter current would excite only sextupole moments and higher.

Comment on AC Mangetic Measurements

Based on the discussion following equation 9, it is apparent that eddy currents can cause a retardation of the magnetic field relative the the applied exitation current of the general form

$$B_y(x,y,t) = \alpha\left[I_0 + \frac{dI}{dt}\left[t - \tau(x,y)\right]\right] \qquad (12$$

where τ is given explicit space dependence. Space dependence of τ leads directly to distortions (i.e. multipole moments) at any instant in time. As dB/dt is independent of τ, however, any magnetic field measuring technique based on flux integration will not measure this τ dependence unless the integration is begun when dI/dt = 0.

In order to know how large the retardation and distortion effects are, AC magnetic field measurements are necessary. They should be carried out in a manner which is sensitive to τ, and without the "warm bore" assembly, which can inject additional distortions into the measurements.

The multipoles can be calculated directly by expanding the above relation in terms of a Taylor series:

$$B_y(x,0,t) = B_y(0,0,t) - \alpha \frac{dI}{dt} \sum_{n=1}^{\infty} \frac{1}{n!} \tau^{(n)}(0,0)\, x^n \qquad (13$$

where $\tau^{(n)}(0,0) = \left.\frac{\partial^n \tau(x,y)}{\partial x^n}\right|_{\substack{x=0 \\ y=0}}$

and $B_y(0,0,t) = \alpha\left[I_o + \frac{dI}{dt}\left[t - \tau(0,0)\right]\right]$

the measurement of $\tau(x,y)$, as it is independent of the level of exitation, possibly could be done by applying a sinewave exitation of a few amps to the terminals of a superconducting magnet and exploring the aperture with a pickup loop. Measurement of $\tau(0,0)$ is done by placing a small air-core inductance in series with the magnet and using it as a reference. Alternately, τ could be measured by measuring the frequency dependence of amplitude as per equation 4. An amplitude measurement of 1 part in 10^4 at 11 Hz would yield a measurement of τ with an accuracy of $\approx$ 70 μsec, however, so perhaps measuring the retardation rather than the attenuation would yield better results.

Conclusion

The above measurements have shown that the major eddy current losses are not in the coils or collars, but in the cryostat assembly. The inductance changes caused by these eddy currents all seem to be at frequencies above 30 Hz or so. Dispersion theory shows that any frequency dependent AC resistance must be reflected in a change in inductance with frequency, so that a precise measurement of inductance vs frequency can predict the AC losses. Furthermore, dispersion theory shows that any frequency dependence of inductance must be reflected in a contribution to the AC resistance. AC losses predicted by these measurements seem to agree with ramp tests made on magnets at high current. Some additional AC magnetic measurements are requested, and some pitfalls of making these measurements are reviewed. In addition, there is a distinct possibility that the stabrite/ebanol insulation problem can be seen. To clarify what to look for, however, it would be useful to know what inductance is excluded when the Nb-Ti filaments become superconducting.

In order to use the simple model (equation 2) in a transmission line analysis of long strings of dipoles, we chosse the value

$$R(\omega) = 1.6 \times 10^{-5} \omega^2 \text{ ohms:}$$

e.g. L = 45 mH

k = 0.6

R = 45 ohms

τ = 600 μsec

In order to compare the power losses during ramping at 400 amps/sec with other forms at power dissipation (such as beam image currents)

$$I^2R = \frac{R(\omega)}{\omega^2}\left(\frac{dI}{dt}\right)^2 = 400^2 \times 1.6 \times 10^{-5} = 2.6 \text{ watts total}$$

$$= 12\% \times 2.6 = 0.3 \text{ watts in bore tube}$$

Appendix: Eddy Currents and Dispersion Relations

It is pointed out in Morse and Feshbach[1] that in general, complex impedances are analytic functions of $x+iy = \omega+i\alpha$, then the real and imaginary components of the impedance are related by dispersion relations. Specifically, the real and imaginary components are not independent but are interrelated in a manner specified by[2]

$$R(\omega) = \frac{-2}{\pi}\int_0^\infty \frac{\omega' X(\omega') - \omega X(\omega)}{\omega'^2 - \omega^2}\, d\omega' \qquad [A\text{-}1]$$

$$X(\omega) = \frac{2\omega}{\pi}\int_0^\infty \frac{R(\omega') - R(\omega)}{\omega'^2 - \omega^2}\, d\omega' \qquad [A\text{-}2]$$

where $Z(\omega) = R(\omega) + j\,X(\omega)$

Forming the subtracted dispersion relation for $R(\omega)$ and substituting $L(\omega) = \frac{X(\omega)}{\omega}$ we get

$$R(\omega) = R(0) - \frac{2\omega^2}{\pi}\int_0^\infty \frac{L(\omega') - L(\omega)}{\omega'^2 - \omega^2}\, d\omega' \qquad [A\text{-}3]$$

where R(o) = the dc resistance of the circuit.

We may divide this integral into two regions $\omega' < \omega$ and $\omega' > \omega$ and integrate by parts:

$$R(\omega) = R(0) - \frac{2\omega^2}{\pi}\int_0^\omega \frac{L(\omega')-L(\omega)}{\omega'^2-\omega^2}\, d\omega' - \frac{2\omega^2}{\pi}\int_\omega^\infty \frac{L(\omega')-L(\omega)}{\omega'^2-\omega^2}\, d\omega' \qquad [A\text{-}4]$$

$$R(\omega) = R(0) + \frac{2\omega^2}{\pi}\int_0^\omega \frac{L(\omega')-L(\omega)}{\omega^2-\omega'^2}\, d\omega' - \frac{2\omega^2}{\pi}\int_\omega^\infty \frac{L(\omega')-L(\omega)}{\omega'^2-\omega^2}\, d\omega' \qquad [A\text{-}5]$$

$$R(\omega) = R(0) - \frac{2\omega}{\pi}\int_0^{\omega} \tanh^{-1}\left(\frac{\omega'}{\omega}\right)\frac{2L(\omega')}{2\omega'}d\omega' - \frac{2\omega}{\pi}\int_{\omega}^{\infty} \coth^{-1}\left(\frac{\omega'}{\omega}\right)\frac{2L(\omega')}{2\omega'}d\omega' \qquad [A-6]$$

the expansions for the hyperbolic circular functions are

$$\tanh^{-1} z = z + \frac{z^3}{3} + \frac{z^5}{5} + \frac{z^7}{7} + \text{-----}$$

$$\coth^{-1} z = \frac{1}{z} + \frac{1}{3z^3} + \frac{1}{5z^5} + \frac{1}{7z^7} + \text{-----} \qquad [A-7]$$

Consider 3 limiting cases:

Case 1 - $\frac{2L(\omega')}{2\omega'} = 0$ everywhere except for $\omega' >> \omega$:

$$R(\omega) = R(0) - \frac{2\omega^2}{\pi}\int_{\omega'>>\omega}^{\infty} \frac{1}{\omega'}\frac{2L(\omega')}{2\omega'}d\omega' \qquad [A-8]$$

i.e. any change in inductance at a frequency $\omega' >> \omega$ gives rise to a term in $R(\omega)$ which is quadratic in ω.

Case 2 - $\frac{2L(\omega')}{2\omega'} = 0$ everywhere except for $\omega' << \omega$:

$$R(\omega) = R(0) - \frac{2}{\pi}\int_0^{\omega'<<\omega} \omega'\frac{2L(\omega')}{2\omega'}d\omega' \qquad [A-9]$$

i.e. any change in inductance at a frequency $\omega' << \omega$ gives rise to a term in $R(\omega)$ which is independent of ω.

Case 3 - $\frac{2L(\omega')}{2\omega'} = 0$ everhwhere except for $\omega' \sim \omega$:

$$R(\omega) \sim R(0) - \frac{2\omega}{\pi} \int_{\omega' \sim \omega} \frac{2L(\omega')}{2\omega'} d\omega' \qquad [A\text{-}10]$$

i.e. any change in inductance at a frequency $\omega' \sim \omega$ gives rise to a term in $R(\omega)$ which is linear in ω. The transition between these limiting cases is continuous (see simple model - equation 2).

It is important to note that as the region where $\frac{2L(\omega')}{2\omega'} \neq 0$ is shifted further and further toward 0 or ∞ (i.e. away from ω in either direction), the maximum contribution the inductance change can made on $R(\omega)$ becomes smaller and smaller. Specifically, if we are interested in $R(\omega)$ for $\omega = 0.1$ to 1 Hz, then a 1 MHy change at 10 Hz is more important than a 10 mHy change at 1000 Hz, or a 1 mHy change at 10^{-4} Hz.

It is important to note the generality of the applicability of dispersion relations:

1. Any frequency dependence of inductance must be accompanied by a corresponding change in resistance.
2. Any frequency dependence of reisitance must be accompanied by a corresponding change in inductance.
3. These statements are not restricted to eddy current losses, or to any particular model. These depend only on the analyticity of the impedance in the $w+i\alpha$ plane.

It should be noted that the specific equations were derived for the case where there are no poles in $L(\omega)$ along the real (ω) axis. Specifically $L(\omega)$ is bounded and positive for all $w>0$. The general conclusions still hold, however. For example a pole of the form $1-\omega^2 LC$ at 5 kHz does not seen to contribute to $R(\omega)$ at 10 Hz.

1. Morse and Feshbach "Methods of Theoretical Physics" (McGraw Hill Book Co.) see section 4.2.

2. Ibid, equation 4.2.21.

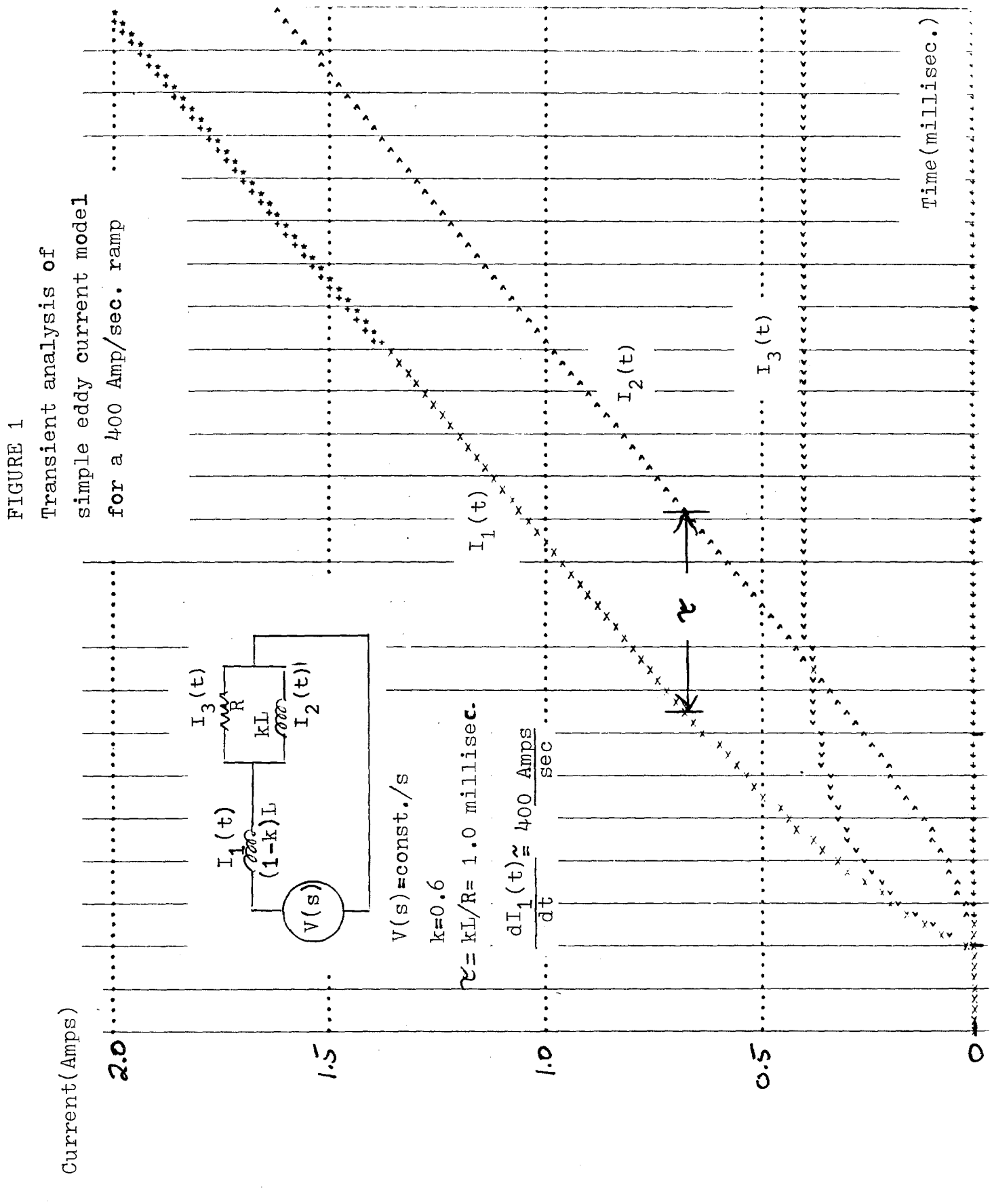

FIGURE 1
Transient analysis of
simple eddy current model
for a 400 Amp/sec. ramp

FIGURE 2A

R(ω) vs. frequency for partially assembled ED dipole coils

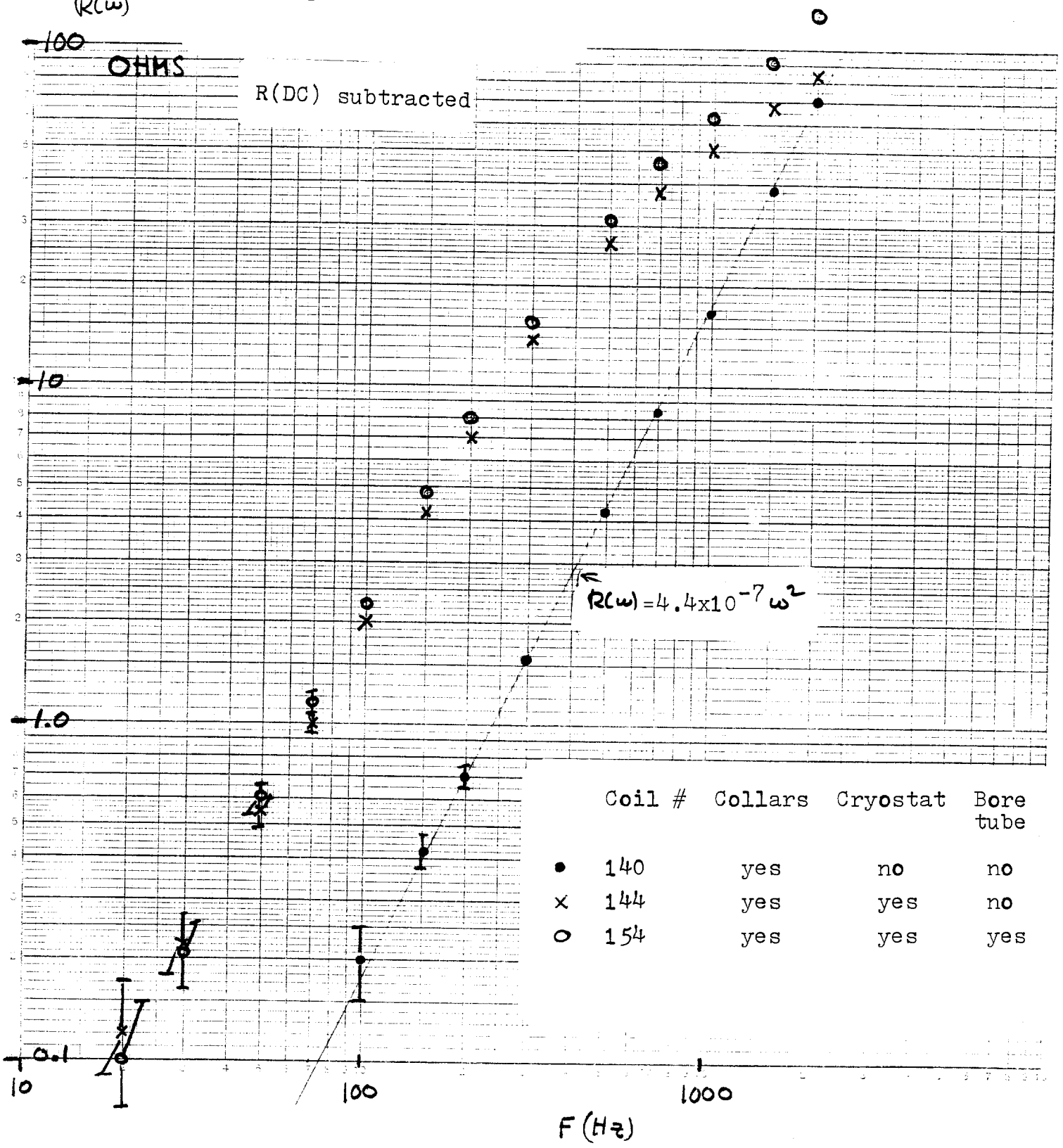

FIGURE 2B

L(ω) vs. frequency for partially assembled ED dipole coils

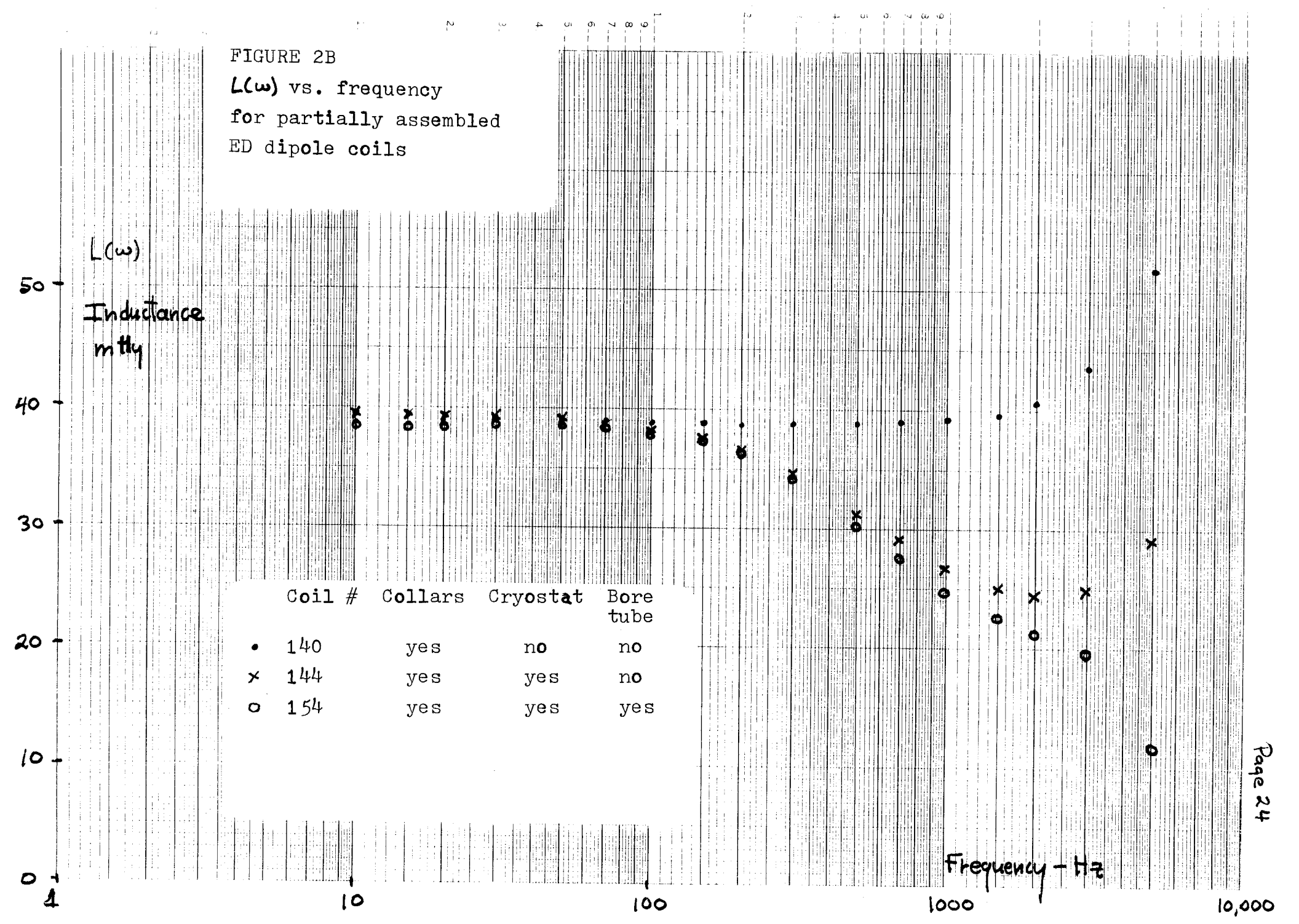

	Coil #	Collars	Cryostat	Bore tube
•	140	yes	no	no
×	144	yes	yes	no
o	154	yes	yes	yes

FIGURE 3A

Coil # 159 in aluminum dewar in Lab 5

R(ω) vs. frequency

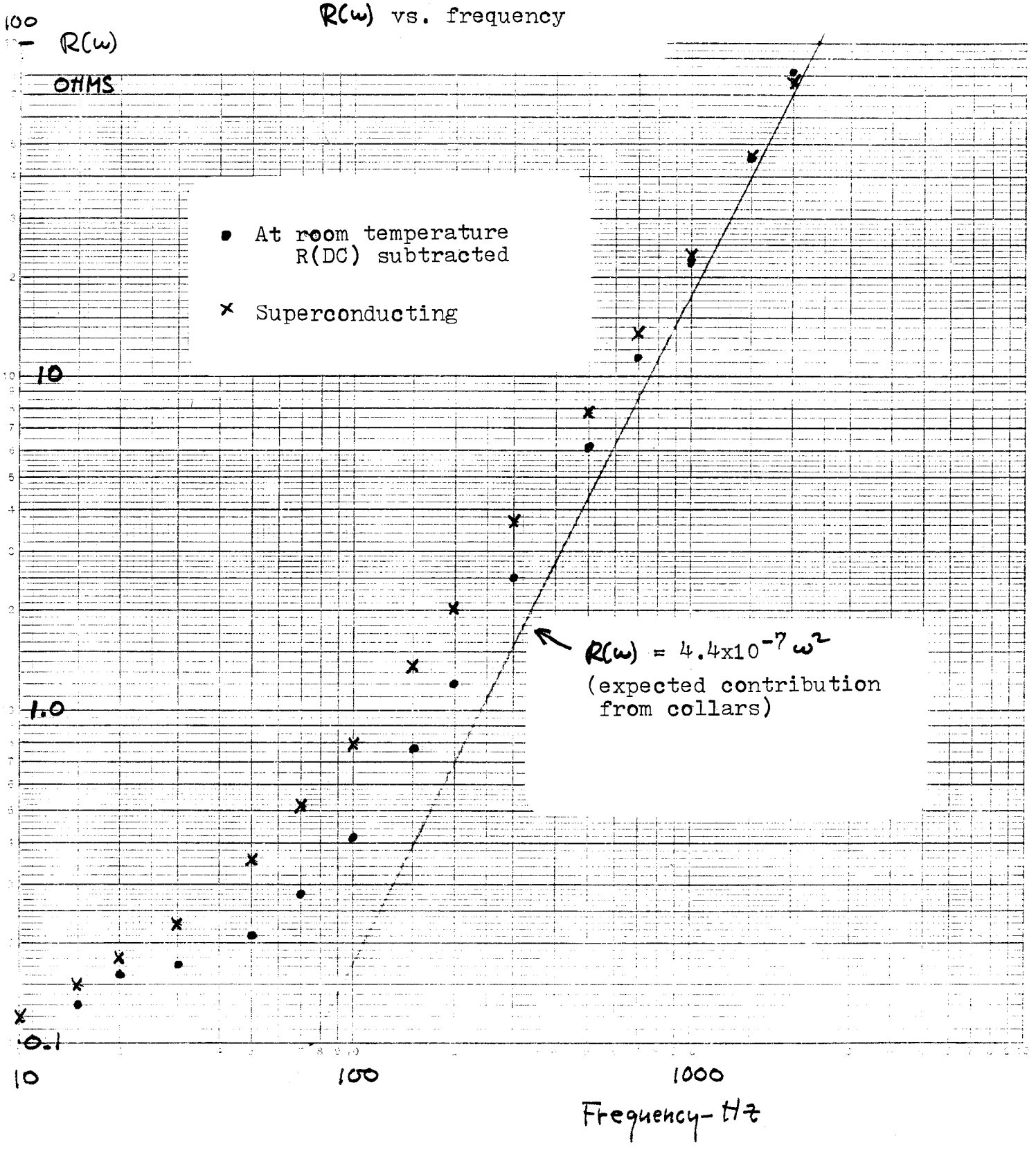

FIGURE 3B

Coil # 159 in aluminum dewar in Lab 5.

L(ω) vs. frequency

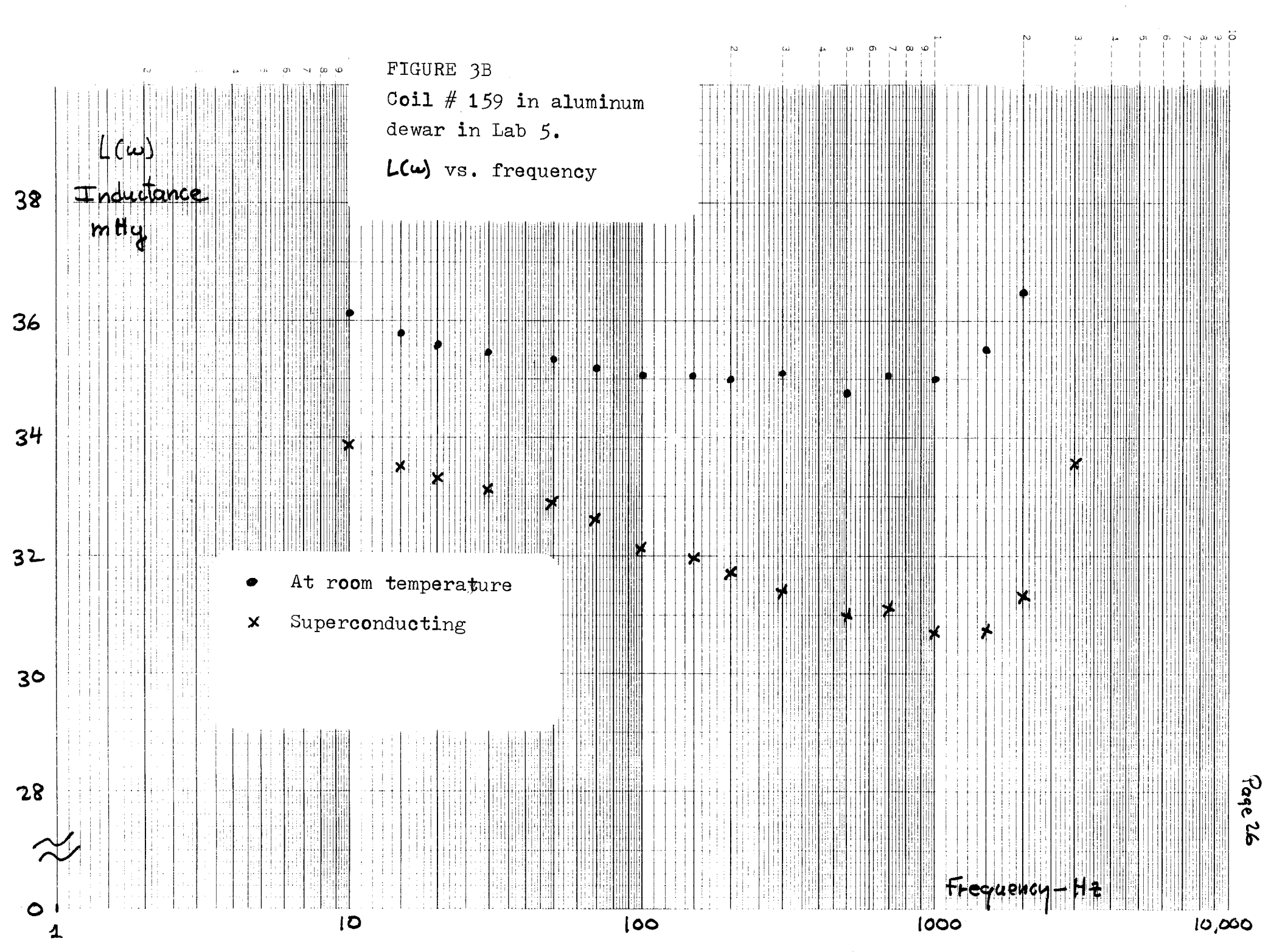

FIGURE 4A

ED dipole magnet #PCA-148
on test stand in
Magnet Factory

R(ω) vs. frequency

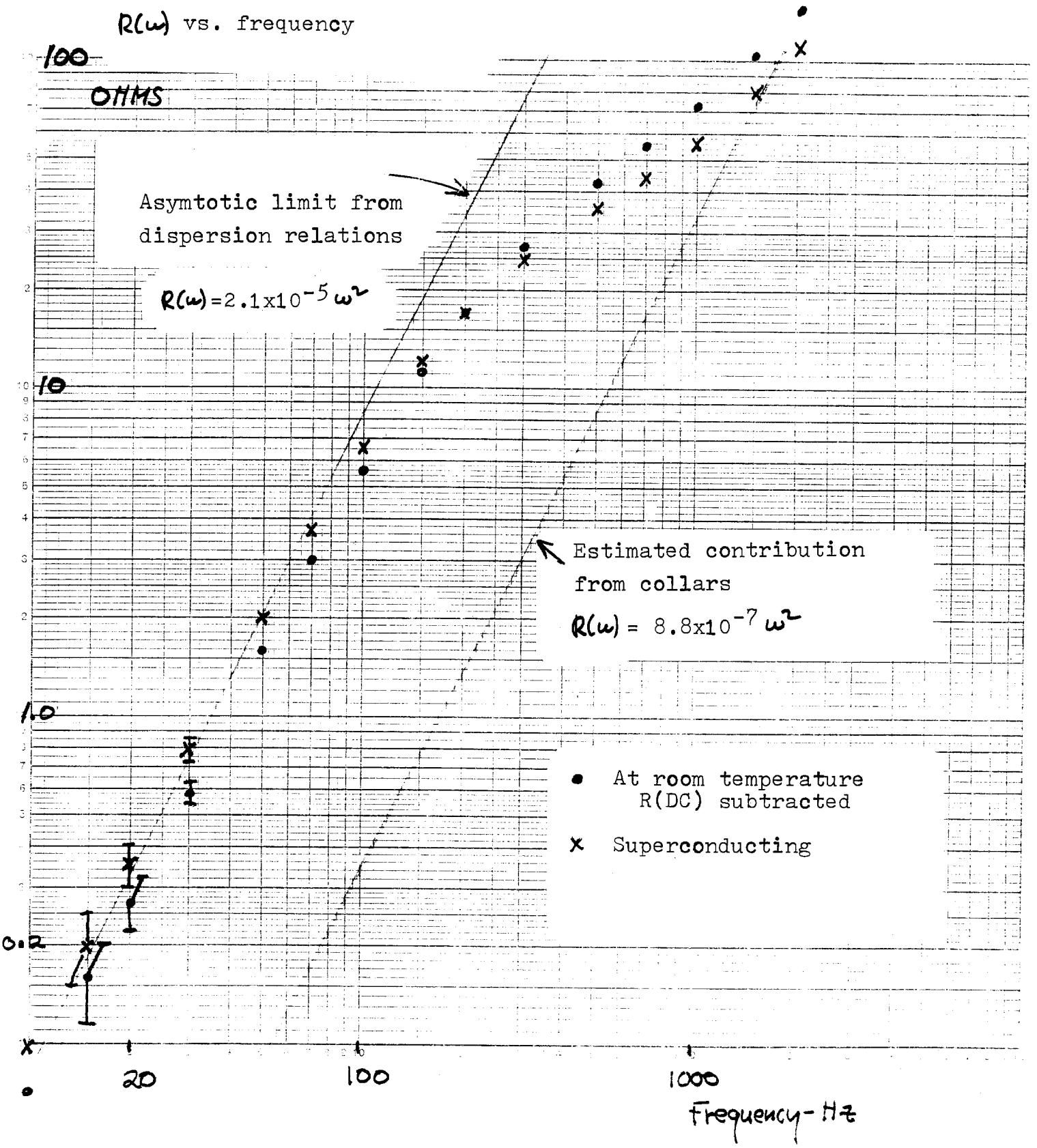

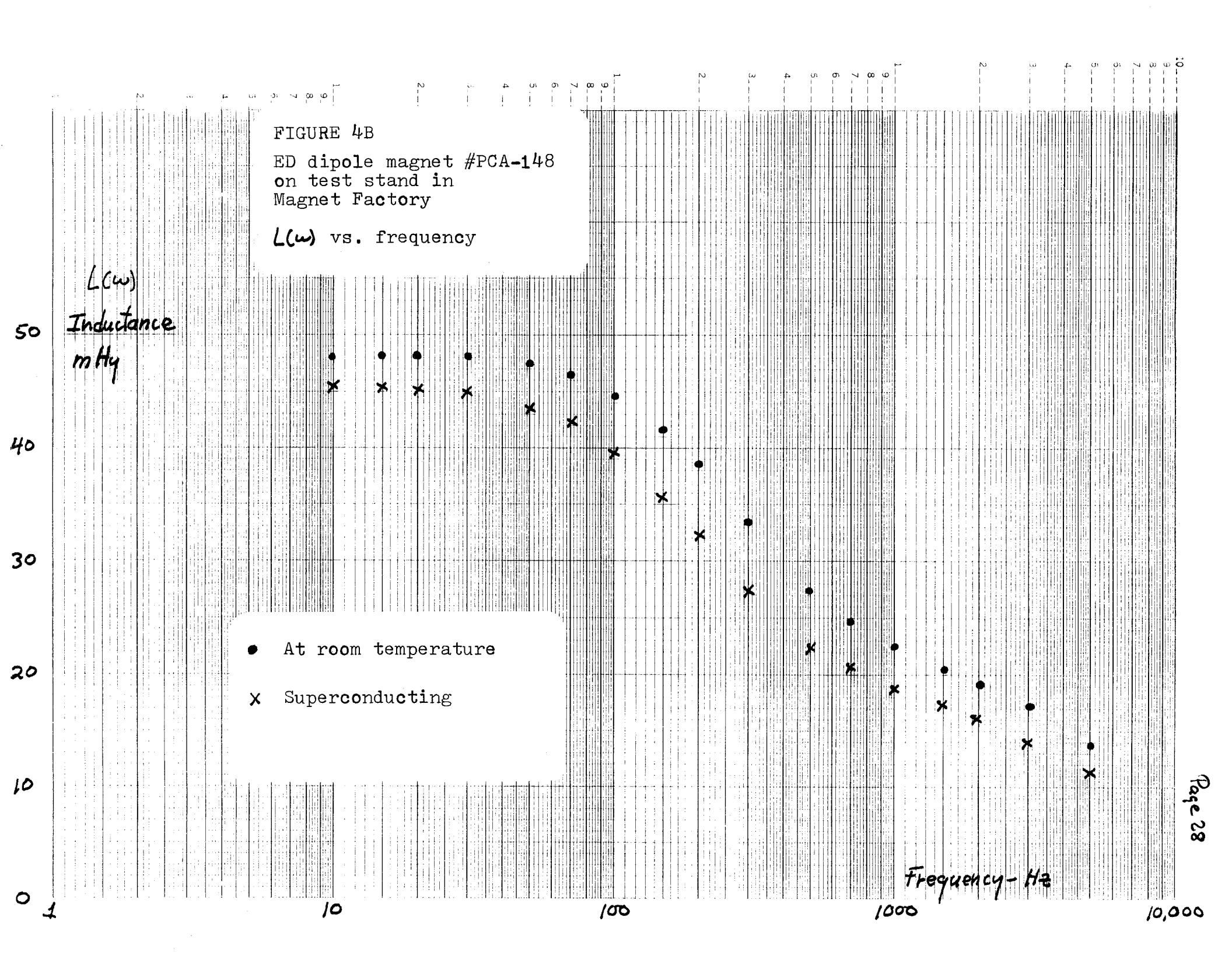
FIGURE 4B
ED dipole magnet #PCA-148
on test stand in
Magnet Factory
L(ω) vs. frequency
L(ω)
Inductance
mHy
50
40
30
20
10
0
1
10
100
1000
10,000
Frequency - Hz
● At room temperature
× Superconducting